CALPHAD formalism for Portland clinker: thermodynamic models and databases

Marie-Noëlle de Noirfontaine, Sandrine Tusseau-Nenez, Caroline Girod-Labianca, V. Pontikis

CALPHAD formalism for Portland clinker: thermodynamic models and databases

M.-N. de Noirfontaine[1,2,*], S. Tusseau-Nenez[2,3], C. Girod-Labianca[2,4], V. Pontikis[2]

[1] *LSI, CNRS UMR 7642 - Ecole Polytechnique, 91128 Palaiseau, France*
[2] *CECM, CNRS UPR 2801, 94407 Vitry-sur-Seine, France*
[3] *ICMPE, CNRS UMR 7182 – Université Paris XII, 94320 Thiais, France*
[4] *CTG-Italcementi Group, les Technodes, 78931 Guerville, France*

Abstract (150-250 words): 239 words

The so-called CALPHAD method is widely used in metallurgy to predict phase diagrams of multi-component systems. The application of the method to oxide systems is much more recent, because of the difficulty of modelling the ionic liquid phase. Since the 1980s, several models have been proposed by various communities. Thermodynamic databases for oxides are available and still under development.

The purpose of this article is to discuss the distinct approaches of the method for the calculation of multi-component systems for Portland cement elaboration. The article gives a state of the art of the most recent experimental data and the various calculations for the CaO-Al_2O_3-SiO_2 phase diagram. A literature review of the three binary sub-systems leads to main conclusions: (i) discrepancies are found in the literature for the selected experimental data, (ii) the phase diagram data in the reference books are not complete and up to date and (iii) the two-sublattices model and the modified quasichemical model can be equally used for the modelling of the aluminates liquid. The predictive feature of the CALPHAD method is illustrated using the CaO-Al_2O_3-SiO_2 system with the two-sublattices model: extrapolated (predicted) and fully-assessed phase diagrams are compared in the clinkering zone of interest. The recent application of the predictive method for the calculations of high-order systems (taking into account Fe_2O_3, SO_3, CaF_2, P_2O_5) shows that the databases developed with the two-sublattices model and the modified quasichemical model are no longer equivalent.

* Corresponding author.
Laboratoire des Solides Irradiés, CNRS UMR 7642, Ecole Polytechnique, 91128 Palaiseau Cedex, France
Tel.: +33 1 69 33 44 83; fax: +33 1 69 33 45 54
e-mail address: marie-noelle.de-noirfontaine@polytechnique.edu

Keywords: *Phase diagrams; thermodynamic calculations; CALPHAD method; Portland cement; clinker*

1. Introduction

Portland cement is obtained by grinding an artificial rock, called the clinker, with a small amount of gypsum (~5%) added in order to delay the setting time of cement. The clinker is produced by heating a mixture of limestone (~80 wt%) and clay (~20 wt%) up to the so-called clinkering temperature (T_c) in the range of 1400-1500 °C. The clinker contains four compounds at least. The two major phases are solid solutions of two calcium silicates, Ca_3SiO_5 and Ca_2SiO_4, referred to as alite and belite, respectively. The two other phases are solid solutions of two calcium aluminates, $Ca_3Al_2O_6$ and $Ca_4Al_2Fe_2O_{10}$. Hereafter, we use the compact mineralogical notation: C=CaO, S=SiO_2, A=Al_2O_3, F=Fe_2O_3. The four compounds are designated as C_3S, C_2S, C_3A and C_4AF.

Understanding the quaternary phase diagram CaO-SiO_2-Al_2O_3-Fe_2O_3 (hereafter referred to as 'CASF' system) is the basis of the chemistry in the kiln. Table 1 summarises the four main zones and successive reactions between 400 °C and T_c. The ternary phase diagram CaO-Al_2O_3-SiO_2 (referred to as 'CAS' phase diagram) is often used for a preliminary understanding of Portland cements. Rankin was the first to determine such a diagram [1]. It is particularly relevant for the fabrication of white cements that are characterised by a very small Fe_2O_3 content. Figure 1 shows the composition area of Portland cements in the 'CAS' system. For white cements, melting temperatures (T_m) and clinkering temperatures (T_c) are about 1380 °C and 1500 °C, respectively. At T_c=1500 °C, the three phases in equilibrium are C_3S, α-C_2S and the aluminates liquid of composition L_c. The respective L_c compositions for 1500 and 1400 °C are: CaO (~59 wt%), Al_2O_3 (~32 wt%), SiO_2 (~9 wt%) and CaO (~55 wt%), Al_2O_3 (~37 wt%), SiO_2 (~8 wt%). In the quaternary 'CASF' system, the temperature of the liquidus is reduced down to T_m=1338 °C. The composition and the proportion of liquid depend on the weight ratio A/F. The proportion of liquid rises up to 15-25 wt% [2]. The Fe_2O_3 proportion in the liquid is in the 5-14 wt% range, for A/F values in the 6.06-0.64 wt% range [3].

The chemistry in the kiln is often modified by the impurities (the so-called minors) introduced during the elaboration process. These impurities are introduced by the rocks, the additives or the fuels. They play an important role during the clinkering process. In some cases, impurities such as SO_3 or MgO change the composition of the interstitial melt [4, 5], leading preferentially to the polymorph M1 or M3 of alite in the clinker [6]. In other cases, minor oxides such as CaF_2 or MgO may lower temperatures T_m and T_c [3], and reduce both the CO_2 emissions and the energy consumption for the fabrication of cement. Since the 1990s, the cement industry has used more and more alternative fuels (ratio up to 1/3), in order to favour the valorization of wastes and reduce the use of fossil fuels. This was the origin of new experimental studies related to the effects of minors, such as phosphorus when meat and bone meals are burnt [7]. These studies highlight the lack of knowledge of multi-component equilibrium phase diagrams. In addition, the knowledge of multi-components phase diagrams for clinker manufacturing is also motivated by the research of new compositions of cement within the context of CO_2 emission reduction.

Table 1 Portland clinker formation: main zones and reactions from 400 °C to 1500 °C in a typical dry-process rotary kiln. In modern plants with preheater towers, the dehydration and initial calcinations take place out of the kiln in the preheater tower.

Zones	T (° C)	Reactions
Dehydration	400- 600	Deshydroxylation of clay (↗ H_2O)
	600- 900	Decomposition of clay, with formation of reactive oxide mixture: SiO_2, Al_2O_3, Fe_2O_3
Calcination	600- 1000	Decomposition of limestone (↗ CO_2) with formation of reactive oxide CaO Formation of C_2S and initial compounds $C_{12}A_7$, CA and C_2F
	1000-1300	Formation of C_2S, C_3A, C_4AF
Clinkering	1320-1380 (T_m)	Melting of C_3A and C_4AF
	1400-1500 (T_c)	Formation of clinker (clinkering) with formation of C_3S: $CaO + C_2S \rightarrow C_3S$ Three phases in equilibrium: $C_3S + C_2S$ + Liquid of aluminates (15-25 wt%)

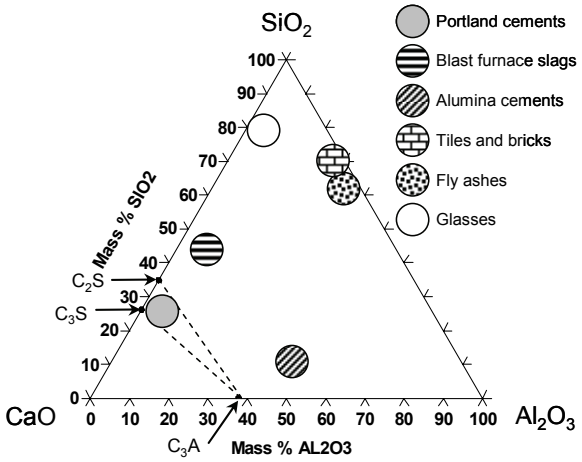

Fig. 1**.** Zone of Portland cements in the 'CAS' system (white cements). Composition of the three arrowed phases: C_3S (wt% SiO_2 = 26.16), C_2S (wt% SiO_2 = 34.88) and C_3A (wt% Al_2O_3 = 37.74).

The most usual approach to determine equilibrium phase diagrams is the experimental route, involving syntheses of samples of various compositions, heat treatments and structural characterisations. Such experimental studies are expensive and time consuming, especially when the number of components of the systems increases. Since the 1970s, an alternative route is to use the computational CALPHAD method (CALculation of PHAse Diagrams) for the modelling of phase diagrams [8, 9].

The CALPHAD method is a semi-empirical method used for the modelling of thermodynamic properties and for the calculation of equilibrium phase diagrams. As far as the molar Gibbs free energies $G_m(x,T,P)$ of all the phases of a given system are known, it becomes possible to calculate the phase diagram by minimising the total Gibbs energy. The molar Gibbs energies of the different phases are given by theoretical thermodynamic models. Then, the parameters of the models are determined by refining a critical set of experimental data using a least-square method and subsequently used for calculating phase diagrams. The determination of the coefficients is often called assessment or optimisation of a system. Since the 1990s, a major effort of the thermodynamic community was to gather data for pure elements and binary mixtures in databases [10]. Even if the determination of the coefficients of binary systems is still time-consuming, the strength of the CALPHAD method lies in its ability to predict ternary or high order systems from the extrapolation of the thermodynamic excess quantities of the sub-systems. With this method, the calculation of high order systems can be reduced down to few minutes. The predominant method, as recommended by Hillert [11], uses an equation developed by Muggianu [12]. Other geometric methods are suitable such as Kohler and Toop's [11, 12].

At the present time, extensive databases exist for metallurgy. The CALPHAD technique is already a routine method for the development of new alloys in metallurgy. Its application to oxide systems is much more recent, mainly because of the difficulty to model the liquid phase. Indeed, ionic liquids exhibit a strong short-range order (SRO) around given compositions. For example, the

silicate melts in the MO-SiO_2 systems with MO basic oxides (M=Ca, Mg, Mn,…) have a strong short order in the vicinity of the molar fraction X_{SiO2}=1/3, which is associated with the formation of orthosilicate compound M_2SiO_4 with congruent melting [13]. Since 1980, four models have been developed: the ionic two-sublattice model [8, 14, 15], the modified quasichemical model [13], the associated model [16] and the cellular model [17]. Various databases for ceramics, geochemistry and steel industry (slags) have been developed with different models and codes. In 2000, the CALPHAD method was applied to cement for the first time: Barry and Glasser [18] performed calculations using the associated model to validate the method for cement clinkering reactions. Since 2000, the thermodynamic community undertook a considerable effort to develop reliable oxide databases. The assessed parameters are published in academic journals or/and gathered into commercial databases. Since 2009, the main databases are: ION3 developed with Thermo-Calc software using the ionic two-sublattice model, FToxid [19] developed with FactSage software using the modified quasichemical model, and NPL oxide developed with MTDATA software using the associated model. These databases are built from the assessed descriptions of all binary constituents systems. Ternary and higher order systems are not always fully optimised, in particular when extrapolation is sufficient to describe the system in the composition and temperature ranges of interest [20]. Based on the available published data, this article aims at pointing out, in the particular composition and temperature domain of clinkering, the possible divergent points and the respective advances of the various databases.

In the first part of the article, the oxide systems of cement interest are reviewed with the aim to compare the assessments arising from several models. The systems discussed are the binary systems: CaO-SiO_2, CaO-Al_2O_3, Al_2O_3-SiO_2 (the knowledge of binaries is a requirement) and the ternary CaO-Al_2O_3-SiO_2 (‘CAS’) system. Then, the predictive power of the method is illustrated on the basis of the CaO-Al_2O_3-SiO_2 system, in particular in the clinkering zone. The article ends with a brief state of the art of the public and commercial thermodynamic databases for taking into account Fe_2O_3 and other components useful for cement industry.

2. Calculation of the three binary sub-systems of the $CaO-Al_2O_3-SiO_2$ system: state-of-art

2.1. A review of the evaluations for the 'CAS' system

Table 2 gives a state of the art of the various evaluations available in the literature for the three binary reference diagrams ($CaO-SiO_2$, $CaO-Al_2O_3$ and $SiO_2-Al_2O_3$) and the ternary $CaO-Al_2O_3-SiO_2$ system. For each assessment, we give the model used for the liquid and the experimental points for the liquidus. It can be seen that the different authors used the four existing models for binaries. For the development of higher order systems, two models only are retained: the two-sublattice model and the modified quasichemical model.

Table 2 Evaluations (or assessments) of the $CaO-Al_2O_3-SiO_2$ ternary phase diagram and its three binary sub-systems. The columns list: (1) the system, (2) the thermodynamic model for the ionic liquid, (3) the thermodynamic calculation software, (4) the selected experimental points for the liquidus, and (5) the reference(s) where the thermodynamic parameters of the phases are described. In columns 4 and 5, the first reference corresponds to the whole selected phase diagram and the following lines give the reinvestigations for some temperature and composition ranges.

System	Model for liquid	Software	Liquidus experimental points	Ref.
$CaO-SiO_2$	Two-sublattice	Thermo-Calc	[21] $T_m(CaO)$ = 2900 °C [22] CaO-rich part: [23] Miscibility gap: [24], [25]	[26], [27], [28]
	Modified quasichemical	FactSage	[1], [29] $T_m(CaO)$ = 2572 °C [30] Miscibility gap: [24], [25]	[31], [13]
	Cellular	Mtdata	[21] $T_m(CaO)$ = 2900 °C [32] CaO-rich part: [23] Miscibility gap: [24], [25]	[33]
	Associated	Bingss	[21] $T_m(CaO)$ = 2900 °C [not mentioned] Miscibility gap: [24], [25]	[34]
	Not mentioned	Ivtanthermo	[21]	[35]

$CaO-Al_2O_3$	Two-sublattice	Thermo-Calc	[36] $T_m(CaO)$ = 2900 °C [22] Liquidus: 49 <wt% Al_2O_3< 51.5 [37] T_m ($C_{12}A_7$) °C = 1392 [38]; 1400 [39]; 1415 [40]; 1455 [1] Liquidus: 64 <wt% Al_2O_3< 100 [41]	[42], [43]
	Modified quasichemical	FactSage	[36] $T_m(CaO)$ = 2572 °C [30] Liquidus: 49 <wt% Al_2O_3< 51.5 [37] Liquidus: 64 <wt% Al_2O_3< 100 [41]	[44]
	Associated	Bingss	[36]	[34]
$Al_2O_3-SiO_2$	Two-sublattice	Thermo-Calc	[45] Liquidus: [46], [47], [48], [49], [50] Field of mullite: [51], [52], [53], [54]	[55]
	Modified quasichemical	FactSage	[45] Field of mullite: [51]	[44]
	Cellular	Thermo-Calc	Same of [55] Liquidus: [56] Invariant equilibria: [57], [58]	[59]
	Associated	FactSage	[60], [45], [47], [51], [57]	[61]
$CaO-Al_2O_3-SiO_2$	Two-sublattice	Thermo-Calc	[21]	[62]
	Modified quasichemical	FactSage	[21]	[13], [44]

2.2. Are the two-sublattice and modified quasichemical models significantly different?

Comparing the analytical expressions involved in the two models, Pelton established that the modified quasi-chemical model (MQM) and the ionic two-sublattice model (also called RILM) are very similar [63]. In this paragraph, we validate this result for the composition range of a Portland clinker.

As shown in the introduction, the liquid of aluminates in Portland clinker is composed of the two main oxides CaO and Al_2O_3. Then, a good description of this liquid requires a good modelling of the liquid of $CaO-Al_2O_3$ phase diagram in a first approximation. The assessments of this phase diagram with the two-sublattice and the modified quasichemical models [43, 44] were both performed

with the same experimental phase diagram information (see Table 2, column 4), except for the choice of the melting temperature of CaO for which a discrepancy of about 300 °C (2900°C versus 2570 °C) is found, depending on the purity of the sample and the experimental method. Figure 2 superimposes the two calculated liquidi together with the experimental liquidus [36]. The two models produce very similar results in the temperature range of clinkerization (1400-1500 °C). Therefore, both models can be equally used. The highest deviation between the calculated liquidus and the experimental liquidus is observed in the CaO-rich part due to the different CaO melting points considered. Indeed, it is important to keep in mind that the assessed functions heavily depend on the choice of the selected experimental data.

In the following of the article, the calculations are performed using the Thermo-Calc software (version S) [64].

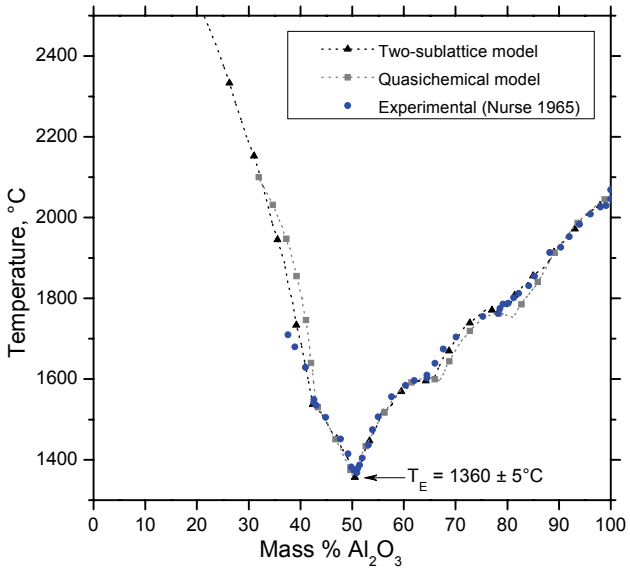

Fig. 2. Liquidus of the CaO-Al_2O_3 system calculated with the two-sublattice model [43] and the modified quasichemical model [44]. The calculated liquidi are compared to the experimental liquidus [36] from 40 to 100 wt% Al_2O_3. T_E = eutectic temperature

2.3. Critical analysis of the 'CAS' binary sub-systems

Based on the assessed Gibbs energies available in literature (Table 2, column 5), Figs. 3, 4 and 5 show the calculated phase diagrams[1] of CaO-SiO_2, CaO-Al_2O_3, SiO_2-Al_2O_3 systems, compared with the experimental data for the liquidi (Table 2, column 4) and the solid phase equilibria. Data from cement reference books are also superimposed. In the following discussion, we point out some experimental disagreements in the literature.

For the CaO-SiO_2 system, the calculated phase diagram (Fig. 3) is compared to the experimental phase diagram of Levin [21] and the further modifications taken into account for the assessment, i.e. the melting temperature of CaO (2900°C instead of 2570°C) [22], the liquidus in the CaO-rich part of the diagram [23] and in the miscibility gap [24, 65]. We insist on the fact that the experimental liquidus reported in the current cement reference books [2, 3] does not include the most recent measurements, the melting point of CaO and the miscibility gap [23]. The measurements of Tewhey and Hess [24] in the miscibility gap seem commonly accepted. The melting temperature of CaO is still controversial (see § 2.2).

For the CaO-Al_2O_3 system, the more recent assessments [43] do not consider the $C_{12}A_7$ phase, since it is not strictly anhydrous [38]. In usual humidity air and in the temperature range 950-1350 °C, the $C_{12}A_7$ phase absorbs small content of water (1.3 wt% at most). For cement phase diagrams, $C_{12}A_7$ is then treated as an aluminate phase i.e. considered as anhydrous, and included in the phase diagrams [2, 3]. The $C_{12}A_7$ phase is an initial compound before the formation of C_3A (Table 1). Figure 4 superimposes the calculated liquidus with most of the experimental data[2] chosen for the assessments [1, 36] (Table 2). Once again, one observes some differences between the selected experimental data and the experimental diagram from Taylor [3], either for the CaO-rich part of the diagram or for the $C_{12}A_7$ compound. Indeed, discrepencies up to 40 °C for the melting temperature of $C_{12}A_7$ can be found in the literature: Taylor and Lea [2, 3]

---

[1] The triangular symbol in the left-hand corner of the diagrams indicates that the figure has been calculated with the Thermo-Calc software. The condensed oxide notation is used for the defined compounds, excepted for the CaO, SiO_2 and Al_2O_3 components.

[2] Note that Rankin firstly assigned the $C_{12}A_7$ phase to C_5A_3.

reported a 1415 °C melting temperature [40], whereas Hallstedt [42] deliberately favoured a 1455 °C melting temperature [1].

For the SiO_2-Al_2O_3 system, many measurements were required for the determination of liquidus and the field phase of mullite (Table 2, Fig. 5). For the mullite phase, no experimental data are available concerning the Al_2O_3-rich side for temperatures below 1500 °C. We emphasize the fact that Mao used a 1545 °C value for the eutectic melting point of cristobalite [46]. A value of 1587 °C [66] is sometimes preferred [44].

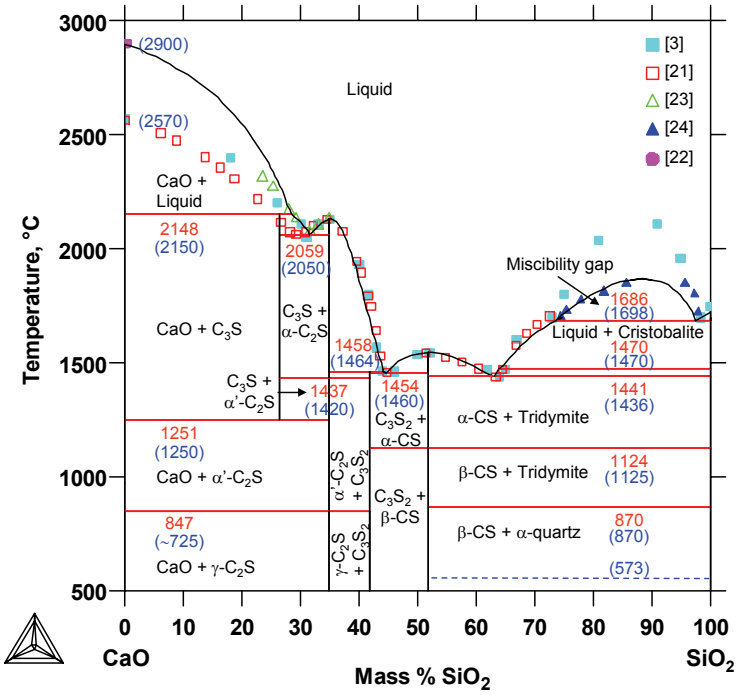

Fig. 3**.** Calculated phase diagram of the CaO-SiO_2 system. The calculated liquidus with the two-sublattice model (black curve) is compared with most experimental data [21,22,23,24] and to the experimental liquidus from Taylor [3]. For the invariant equilibria (horizontal lines), the calculated temperatures are compared with the experimental ones written in parentheses. The experimental equilibrium at T=573 °C (dotted line) is not calculated because the β-quartz polymorph of SiO_2 is not taken into account.

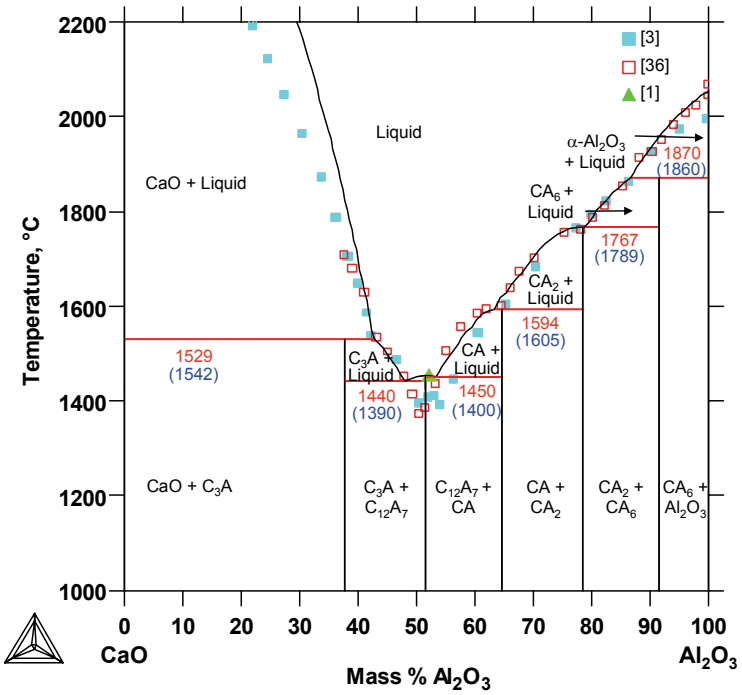

Fig. 4. Calculated phase diagram of the CaO-Al_2O_3 system. The calculated liquidus with the two-sublattice model (black curve) is compared with most experimental data [1, 36] and with the experimental liquidus from Taylor [3]. For the invariant equilibria (horizontal lines), the calculated temperatures are compared with the experimental ones (in parentheses).

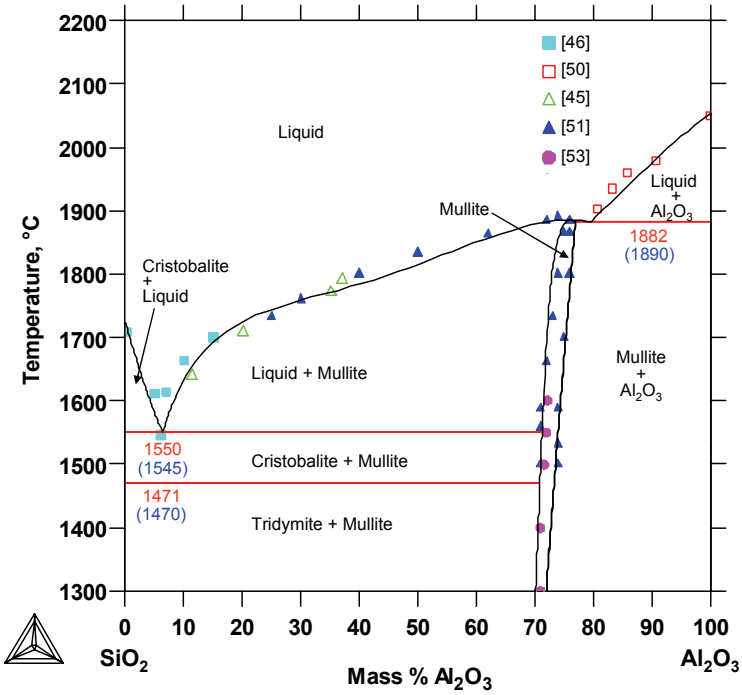

Fig. 5. Calculated phase diagram of the SiO_2-Al_2O_3 system compared to most experimental data [45, 46, 50, 51, 53] (Table 2). For the invariant equilibria (horizontal lines), the calculated temperatures are compared with the experimental ones (in parentheses).

3. The CALPHAD method: a predictive tool for the thermodynamics of clinkers?

The main interest of the CALPHAD method is its ability to predict a ternary system from well-evaluated binary sub-systems. The efficiency of this method is illustrated here for the prediction of the 'CAS' system in the temperature and composition ranges of the clinkering zone (Table 1). In this section, we compare the phase diagram calculated by means of the extrapolation method of Muggianu to the fully optimized phase diagram evaluated by Mao et al. (Table 2). The results are shown as isothermal sections at T=1400 and 1500 °C. The calculations are carried out without taking into account the $C_{12}A_7$ phase, to better compare our results to those of Mao et al. [62].

In a first step, we calculate the 'CAS' ternary liquid using the extrapolation method of Muggianu; the knowledge of the three binary sub-systems is sufficient here. No ternary terms are added. The ionic liquid is described by the two following sublattices: $(Ca^{2+}, Al^{3+})_P(AlO_2^-, O^{2-}, SiO_4^{4-}, SiO_2,)_Q$. Figure 6a and c show the results of extrapolations for 1400 and 1500 °C, respectively. The calculated liquidus is compared to Rankin experimental liquidus [1]. The 'C' zone defined in Fig. 1 reports the typical clinkering zone of a Portland cement. Even if the 'C' zone is the only zone of interest in this study, the whole range of composition is reported for a global discussion of the CALPHAD approach. Hereafter, we will distinguish the field of the liquid of aluminates at the poor-SiO_2 part of the diagram (0-15 wt% SiO_2) from the field(s) of liquid in the richer-SiO_2 part of the diagram (20-90 wt% SiO_2). They will be respectively referred to as 'A-liquid' and 'S-liquid' fields.

In the 'C' zone, the predicted phases in equilibrium are as expected: C_3S, C_2S and the 'A-liquid' of composition L_c (Table 1), noted 'A-liquid(L_c)'. C_2S polymorphs are respectively α' and α for 1400 and 1500 °C. Considering the experimental uncertainty (see footnote of Table 2), the calculated composition L_c, L_c(calc), is overestimated by about 3-4 wt% SiO_2 and underestimated by about 5 wt% Al_2O_3 with respect to the Rankin L_c(exp) experimental composition [1] (Table 3). However, the shape of the liquidus is quite well reproduced.

Outside the clinkering zone, in the richer-SiO_2 part of the diagram, the liquidus of 'S-liquid' is not well reproduced. It shows that the strong ternary interactions (ternary solid compounds, ternary liquid interactions) that exist in this region of the phase diagram should be taken into account. In 2006, Mao et al. evaluated anorthite (A) and gehlenite (G), both ternary solid compounds outside the clinkering zone of interest, and also the ternary interactions of the liquid.

In the second step, all the parameters of the fully optimised system of Mao are now considered (Fig. 6b, d). In this step, no change is found in the 'A-liquid', but the 'S-liquid' is now well reproduced. Indeed, Mao et al. essentially focused on the 'S-liquid' field, in order to get a proper description of the liquid miscibility gap in the ternary system.

The compositions L_c(calc) calculated from extrapolation or from the full optimisation are given in Table 3. The value of L_c(calc) is not sensitive to the addition of any ternary interactions. Table 4 gives the resulting proportions for a typical white Portland clinker (70 wt% CaO, 25 wt% SiO_2 and 5 wt% Al_2O_3). The major differences are observed for the proportions of the C_2S and liquid phases, with a maximum difference about 4.5% for T=1500 °C.

In conclusion, the prediction of the ternary 'CAS' phase diagram with the extrapolation method is relevant in the clinkering zone of interest. All the compositions, that of the 'A-liquid' and those of the three phases in equilibrium, can be estimated with a reasonable accuracy. If more precision is required for the 'A-liquid' in the clinkering zone, the assessment of Mao *et al.* can be improved by additional measurements in this zone, such as those of activities of Al_2O_3 in the liquid.

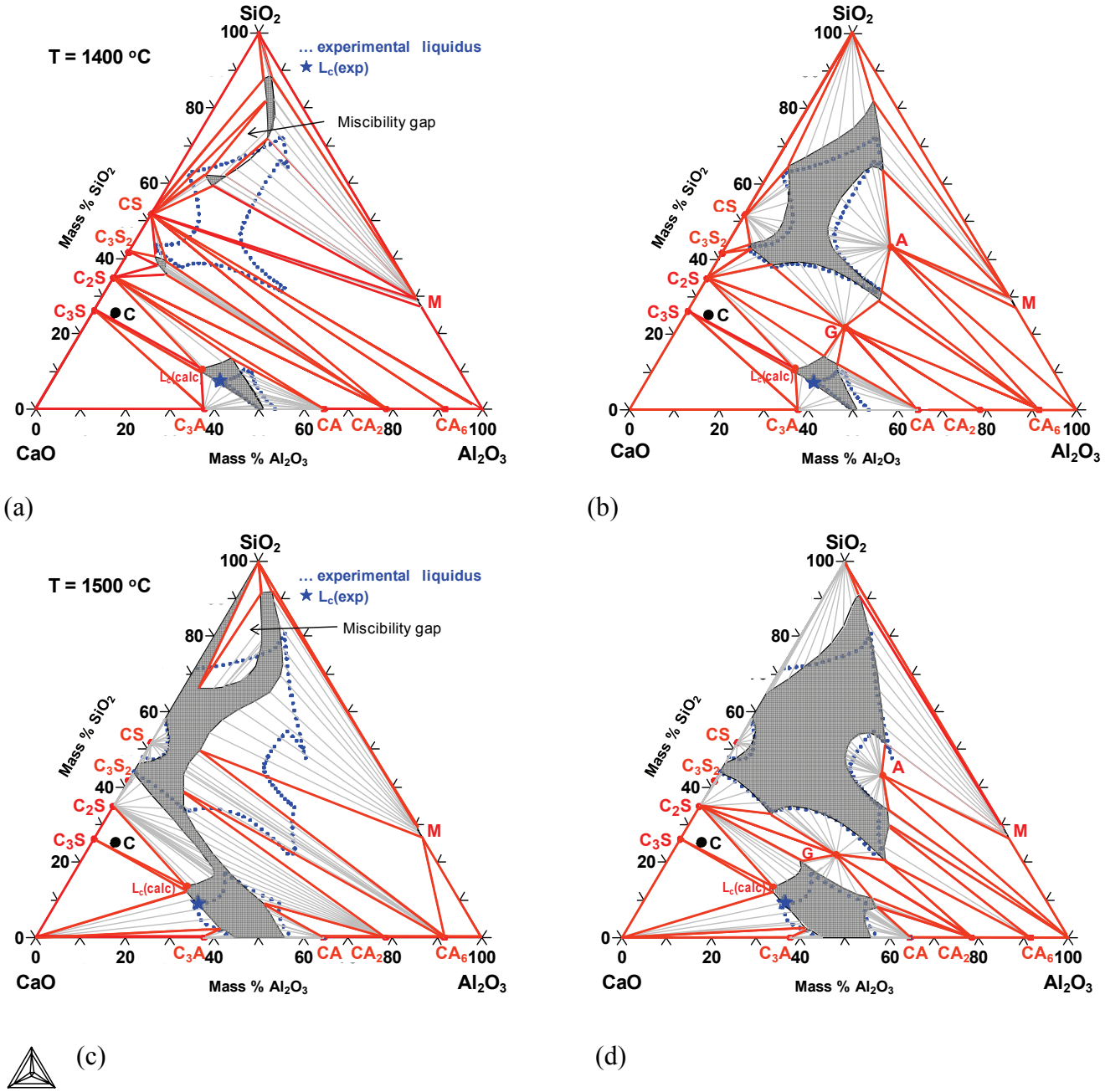

Fig. 6. Isothermal sections at T=1400 °C (a, b) and T=1500 °C (c, d) issued from the calculations of the 'CAS' system. The grey lines are the tie lines of two-phase equilibrium fields, and the other thick lines delimitate the three-phase equilibrium fields. The grey-coloured domains are the liquid fields. The dotted lines show the experimental liquidus [1]. The 'C' zone designates the typical clinkering zone of Portland cement (Fig. 1). L_c(calc) and L_c(exp) are respectively the calculated and experimental compositions of the liquid of aluminates (A-liquid) in the clinkering zone. M = Mullite. (a, c) calculation of the 'CAS' system from the Muggianu extrapolation (b, d) adding the ternary interactions: gehlenite and anorthite solid phases, and the ternary liquid interactions.

Table 3

Calculated composition $L_{c(calc)}$ of the liquid of aluminates in equilibrium with C_3S and C_2S at T=1400 °C and T=1500 °C, with the two steps of calculations of Fig. 6. The last column gives the Rankin experimental composition L_c(exp) deduced graphically [1].

		L_c(calc)		L_c(exp)
	Step	(extrapolation)	(assessment)	
T=1400 °C	wt% CaO	57.7	57.7	55
	wt% Al_2O_3	31.8	31.8	37
	wt% SiO_2	10.5	10.5	8
T=1500 °C	wt% CaO	59.5	59.5	59
	wt% Al_2O_3	26.9	26.9	32
	wt% SiO_2	13.6	13.6	9

Table 4

Calculated and experimental proportions (wt%) of the three phases in equilibrium Liquid(L_c) + C_2S + C_3S at T=1400 °C and T=1500 °C, for a given white Portland clinker of composition 70 wt% CaO, 25 wt% SiO_2 and 5 wt% Al_2O_3. The experimental proportions are estimated with the lever rule from the Rankin experimental diagram [1].

	wt%	Calc.	Exp.
T=1400 °C	Liquid (L_c)	15.7	13
	α'-C_2S	14.8	16
	C_3S	69.5	71
T=1500 °C	Liquid (L_c)	18.6	14
	α-C_2S	12.1	16
	C_3S	69.3	70

5. Towards thermodynamic databases for cement materials

This last part compares advances of the available oxide databases developed with the three models (associated, modified quasichemical and ionic two-sublattice models) to compute the quaternary system CaO-SiO_2-Al_2O_3-Fe_2O_3 ('CASF') and to take into account minor oxides such as MgO, SO_3, P_2O_5 and alkalis.

The calculation of the quaternary phase diagram 'CASF' requires the knowledge of the 'CAS' system and the three other ternary phase diagrams: CaO-Al_2O_3-Fe_2O_3, CaO-SiO_2-Fe_2O_3, and Al_2O_3-Fe_2O_3-SiO_2. All the three binary sub-systems (CaO-Fe_2O_3, Al_2O_3-Fe_2O_3, and SiO_2-Fe_2O_3) have been fully optimized

with the three models [18, 67-69] except the Al_2O_3-Fe_2O_3 system that has not been evaluated yet with the two-sublattice model (ION3 database). FToxid database recently included Fe_2O_3: the ternary solid compound C_4AF is modelled and the ternary and higher order liquids are well extrapolated. NPL oxide database takes into account Fe_2O_3 as well as for C_4AF as for the liquid.

For the case of MgO oxide, data are available in the literature. The three ternary systems Al_2O_3-CaO-MgO, Al_2O_3-MgO-SiO_2 and CaO-MgO-SiO_2 have been fully assessed, both with the two-sublattice model [28, 70, 71] and the modified quasichemical model [72, 73]. As far as there is no quaternary solid compound stabilized in the Portland clinker zone, extrapolation to the quaternary system CaO-Al_2O_3-SiO_2-MgO is applied in the various databases.

For the other minor oxides of interest, the situation is very different. Because the modelling of oxides and commercial interests are still recent, no optimized data for the binary phase diagrams of CaO, SiO_2 or Al_2O_3 with SO_3, CaF_2 or P_2O_5 have been published. However, FT-oxid database has recently included SO_3 [19], CaF_2 and alkalis (Na_2O, K_2O) and can be used for cement industry. The Gibbs energy modelling of phosphate phases is already in progress and need further investigations.

6. Conclusion

Based on a literature review, we have pointed out that some discrepancies still remain concerning several melting points and that the phase diagram data in the current cement reference books are not complete and up to date. We have also shown that both the two-sublattices model and the modified quasi-chemical model for liquids are relevant up to the calculation of the ternary CaO-Al_2O_3-SiO_2 ('CAS') system. Differences between the calculations depend on the choice of the selected experimental data for the assessments. The predictive feature of the CALPHAD method for the calculation of multi-component phase diagrams is illustrated on the 'CAS' ternary phase diagram. As there are no strong

ternary interactions in the clinkering zone of interest, a relevant preliminary phase diagram can be obtained from extrapolation. This predictive method appears as a useful tool to estimate the composition L_c and the proportion of liquid in the clinkering zone. For the time being, the composition L_c can be obtained with average deviations from experiments of about 3-4 wt% SiO_2 and 5 wt% Al_2O_3. Additional assessments ought to be performed for a better accuracy around the L_c composition.

The CALPHAD methodology is applied in commercial databases (NPL oxide, FToxid and ION3) for further calculations of higher order systems, in particular including Fe_2O_3, MgO, SO_3, P_2O_5 and alkalis. Considering the data published up to now, the thermodynamic modelling of iron (or other minor elements)-containing liquids have not reached the same level of relevance for the three models. Since a decade, Factsage and MTDATA communities develop the most extensive databases for cement industry, based on the associated and modified quasichemical models.

Acknowledgements

CTG-Italcementi Group financially supported this study, within the research collaboration framework between the CECM (CNRS, France) and CTG (Italcementi Group, France) laboratories. The authors acknowledge B. Bollotte, E. Moudilou and F. Amin (CTG) for valuable discussions. Many thanks to G. Inden, Bo Sundman, J.-M. Joubert and P. Chartrand for fruitful discussions about Calphad method, models and softwares. The authors also express their sincere thanks to H. Szwarc and R. Céolin for advice and are warmly thankful to F. Dunstetter for his critical reading of the manuscript.

References

1. Rankin GA, Wright FE (1915) The ternary system CaO-Al_2O_3-SiO_2. American Journal of Sciences 39:1-79
2. Lea F (1998) Lea's Chemistry of Cement and Concrete. Fourth edition. P.C. Hewlett, London
3. Taylor HFW (1997) Cement Chemistry. 2nd edition, Thomas Telford Edition, London
4. Butt YM, Timashev VV The mechanism of clinker formation processes and the modification of its structure. In: 6th International Congress on the Chemistry of Cement, Moscow, September 1974 1974. pp 2-43

5. Timashev VV Cinétique de la clinkérisation. Structure et composition du clinker et ses phases. In: 7th International Congress on the Chemistry of Cement, Paris, 1980. pp 1-19
6. Maki I, Goto K (1982) Factors influencing the phase constitution of alite in Portland cement clinker. Cement and Concrete Research 12:301-308
7. de Noirfontaine M-N, Tusseau-Nenez S, Signes-Frehel M, Gasecki G, Girod-Labianca C (2009) Effect of Phosphorus Impurity on Tricalcium Silicate T_1: From Synthesis to Structural Characterization. Journal of the American Ceramic Society 92 (10):2337-2344
8. Saunders N, Miodownik AP (1998) CALPHAD (Calculation of the Phase Diagrams): A comprehensive Guide. Pergamon materials series, Oxford
9. Lukas HL, Fries SG, Sundman B (2007) Computational Thermodynamics. The Calphad method. Cambridge University Press, New-York
10. Special issue of Calphad journal (1995), vol 19 (4): 433-575
11. Hillert M (1980) Empirical methods of predicting and representing thermodynamic properties of ternary solution phases. Calphad 4 (1):1-12
12. Muggianu Y-M, Gambino M, Bros J-P (1975) Enthalpies de formation des alliages liquides bismuth-étain-gallium à 723 K. Choix d'une représentation analytique des grandeurs d'excès intégrales et partielles de mélange. Journal de Chimie Physique 72:83-88
13. Pelton AD, Blander M (1986) Thermodynamic analysis of ordered liquid solutions by a modified quasichemical approach - Application to the silicate slags. Metallurgical Transactions B 17:805-815
14. Hillert M, Jansson B, Sundman B, Agren J (1985) A two-sublattice model for molten solutions with different tendency for ionization. Metallurgical Transactions A 16:261-266
15. Sundman B (1991) Modification of the two-sublattice model for liquids. Calphad 15 (2):109-119
16. Sommer F (1982) Association model for the description of the thermodynamic functions of liquid alloys. Zeitschrift für Metallkunde 73 (2):72-76
17. Gaye H, Welfringer J Modelling of the thermodynamic properties of complex metallurgical slags. In: Metallurgical slags and fluxes, 2nd International Symposium, Warrendale, 1984. pp 357-375
18. Barry TI, Glasser FP (2000) Calculations of Portland cement clinkering reactions. Advances in Cement Research 12 (1):19-28
19. Decterov SA, Kang Y-B, Jung I-H (2009) Thermodynamic Database for the Al-Ca-Co-Cr-Fe-Mg-Mn-Ni-Si-O-P-S System and Applications in Ferrous Process Metallurgy. Journal of Phase Equilibria and Diffusion 30 (5):443–461
20. Kattner UR, Handwerker CA (2001) Calculation of phase equilibria in candidate solder alloys. Zeitschrift für Metallkunde 92 (7):740-746
21. Levin EM, Robbins CR, McMurdie HF (1964) Phase diagrams for ceramists. The American Ceramic Society, Columbus, Ohio
22. Yamada T, Yoshimura M, Somiya S (1986) Reinvestigation of the solidification point of CaO by digital pyrometry. Journal of the American Ceramic Society 69 (10):C243-245
23. Levin EM, McMurdie HF (1975) Phase diagrams for ceramists 1975 supplement. The American Ceramic Society, Columbus, Ohio
24. Tewhey JD, Hess PC (1979) The two phase region in the CaO-SiO_2 system: experimental data and thermodynamic analysis. Physics and Chemistry of Glasses 20 (3):41-52

25. Hageman VBM, Van den Berg GJK, Janssen HJ, Oonk HAJ (1986) A reinvestigation of liquid immiscibility in the SiO_2-CaO system. Physics and Chemistry of Glasses 27 (2):100-105
26. Hillert M, Sundman B, Wang X (1990) An assessment of the CaO-SiO_2 System. Metallurgical Transactions B 21:303-312
27. Hillert M, Sundman B, Wang X (1991) A reevaluation of the rankinite phase in the CaO-SiO_2 system. Calphad 15 (1):53-58
28. Huang WL, Hillert M, Wang X (1995) Thermodynamic assessment of the CaO-MgO-SiO_2 system. Metallurgical Transactions A 26:2293-2310
29. Tromel G, Fix W, Heinke R (1969) Hochtemperaturuntersuchungen bis 1900°C an Calciumorthosilikat und Tricalciumsilikat Tonindustrie-Zeitung 93-1:1-8
30. Elliott JF, Gleiser M (1960) Thermochemistry for steelmaking. Addison-Wesley, MA, United States
31. Eriksson G, Wu P, Blander M, Pelton AD (1994) Critical Evaluation and Optimization of the Thermodynamic Properties and Phase Diagrams of the MnO-SiO_2 and CaO-SiO_2. Canadian Metallurgical Quarterly 33 (1):13-21
32. Somiya S. Unpublished work, Tokyo Inst. Technology, Yokahama
33. Taylor JR, Dinsdale AT (1990) Thermodynamic and phase diagram data for the CaO-SiO_2 system. Calphad 14 (1):71-88
34. Ball RGJ, Mignanelli MA, Barry TI, Gisby JA (1993) The calculation of phase equilibria of oxide core-concrete systems. Journal of Nuclear Materials 201:238-249
35. Zaitsev AI, Zemchenko M, Litvina AD, Mogutnov BM (1993) Thermodynamic calculation of phase equilibria in the CaF_2-SiO_2-CaO system. Journal of Materials Science 3 (5):541-546
36. Nurse RW, Welch JH, Majumdar AJ (1965) The CaO-Al_2O_3 System in a Moisture-free Atmosphere. Transactions and Journal of the British Ceramic Society 64:409-418
37. Nityanand N, Fine HA (1983) The effect of TiO_2 additions and oxygen potential on liquidus temperatures of some CaO-Al_2O_3 melts. Metallurgical and Materials Transactions B 14 (4):685-692
38. Nurse RW, Welch JH, Majumdar AJ (1965) The 12CaO.7Al_2O_3 phase in the CaO-Al_2O_3 System. Transactions and Journal of the British Ceramic Society 64:323-332
39. Muan A, Osborn EF (1965) Phase equilibria among oxides in steel-making. Addison-Wesley, Reading, Massachusetts
40. Chatterjee AK, Zhmoidin GI (1972) The phase equilibrium diagram of the system CaO-Al_2O_3-CaF_2. Journal of Material Science 7:93-97
41. Rolin M, Thanh PH (1965) Les diagrammes de phases des mélanges ne réagissant pas avec le molybdène. Revue des Hautes Températures et Réfractaires 2:175-185
42. Hallstedt B (1990) Assessment of the CaO-Al_2O_3 System. Journal of the American Ceramic Society 73 (1):15-23
43. Mao H, Selleby M, Sundman B (2004) A re-evaluation of the liquid phases in the CaO-Al_2O_3 and MgO-Al_2O_3. Calphad 28:307-312
44. Eriksson G, Pelton AD (1993) Critical evaluation and optimization of the thermodynamic properties and phase diagrams of the CaO-Al_2O_3, Al_2O_3-SiO_2, and CaO-Al_2O_3-SiO_2 systems. Metallurgical Transactions B 24:807-816
45. Aramaki S, Roy R (1962) Revised Phase Diagram for the System Al_2O_3-SiO_2. Journal of the American Ceramic Society 45 (5):229-242

46. Bowen NL, Greig JW (1924) The system: Al_2O_3.SiO_2. Journal of the American Ceramic Society 7 (4):238-254
47. Aksay IA, Pask JA (1975) Stable and metastable equilibria in the system SiO_2-Al_2O_3. Journal of the American Ceramic Society 58 (11-12):507-512
48. Davis RF, Pask JA (1972) Diffusion and reaction studies in the system Al_2O_3-SiO_2. Journal of the American Ceramic Society 55 (10):525-531
49. Konopicky K (1956) Remarques relatives au diagramme d'equilibre SiO_2-Al_2O_3. Bulletin de la Société française de Céramiques 33:3-6
50. Toropov NA, Galakhov FY (1951) New data on the system Al_2O_3-SiO_2. Doklady Akademii Nauk SSSR 78 (2):299-302
51. Klug FJ, Prochazka S, Doremus RH (1987) Alumina-silica phase diagram in the mullite region. Journal of the American Ceramic Society 70 (10):750-759
52. Hamano K, Sato T, Nakagawa Z (1986) Properties of mullite powder prepared by coprecipitation and microstructure of fired bodies. Yogyo-Kyokai-Shi 94 (8):818-822
53. Okada K, Otsuka N (1987) Change in chemical composition of mullite formed from $2SiO_2.3Al_2O_3$ xerogel during the formation progress. Journal of the American Ceramic Society 70 (10):C245–247
54. Prochazka S, Klug FJ (1983) Infrared-transparent mullite ceramic. Journal of the American Ceramic Society 66 (12):874-880
55. Mao H, Selleby M, Sundman B (2005) Phase equilibria and thermodynamics in the Al_2O_3-SiO_2 system - Modelling of mullite and liquid. Journal of the American Ceramic Society 88 (9):2544-2551
56. Risbud SH, Pask JA (1978) Mullite crystallization from SiO_2-Al_2O_3 melts. Journal of the American Ceramic Society 61 (1-2):63-67
57. Horibe T, Kuwabara S (1967) Thermo-analytical investigation of the phase equilibria in the Al_2O_3-SiO_2 system. Bull. Chem. Soc. Jpn. 40 (4):972-982
58. Staronka A, Pham H, Rolin M (1968) Etude du système silice-alumine par la méthode des courbes de refroidissement. Revue Internationale des Hautes Températures et des Réfractaires 5:111-115
59. Fabrichnaya OB, Costa e Silva A, Aldinger F (2004) Assessment of thermodynamic functions in the MgO-Al_2O_3-SiO_2 system. Zeitschrift für Metallkunde 95 (9):793-805
60. Welch JH (1960) A new interpretation of the mullite problem. Nature 186:545-546
61. Yazhenskikh E, Hack K, Müller M (2008) Critical thermodynamic evaluation of oxide systems relevant to fuel ashes and slags. Part 3: Silica–alumina system. Calphad 32:195-205
62. Mao H, Hillert M, Selleby M, Sundman B (2006) Thermodynamic assessment of the CaO-Al_2O_3-SiO_2 system. Journal of the American Ceramic Society 89 (1):298-308
63. Pelton AD (2005) Thermodynamic models and databases for slags, fluxes and salts. Mineral Processing and Extractive Metallurgy (Trans. Inst. Min. Metall. C) 114:C172-180
64. Andersson JO, Helander T, Hoglund L, Shi P, Sundman B (2002) Thermo-Calc & Dictra, Computational Tools for Materials Science. Calphad 26 (2):273-312
65. Roth RS, Dennis JR, McMurdie HF, Clevinger MA, Ondik HM, Schenk PK (1987) Phase diagrams for ceramists. The American Ceramic Society, Westerville, Ohio

66. Schairer JF, Bowen NL (1955) The system K_2O-Al_2O_3-SiO_2. American Journal of Science 253:681-746
67. Hillert M, Selleby M, Sundman B (1990) An assessment of the Ca-Fe-O System. Metallurgical Transactions A 21:1990-2759
68. Fabrichnaya OB, Sundman B (1997) The assessment of thermodynamic parameters in the Fe-O and Fe-Si-O systems. Geochimica et Cosmochimica Acta 61 (21):4539-4555
69. Decterov SA, Jung IH, Jak E, Kang YB, Hayes P, Pelton AD Thermodynamic modelling of the Al_2O_3-CaO-CoO-CrO-Cr_2O_3-FeO-Fe_2O_3-MgO-MnO-NiO-SiO_2-S system and applications in ferrous process metallurgy. In: VII International Conference on Molten Slags Fluxes and Salts, 2004. The South African Institute of Mining and Metallurgy, pp 839-850
70. Hallstedt B (1995) Thermodynamic Assessment of the CaO-MgO-Al_2O_3. Journal of the American Ceramic Society 78 (1):193-198
71. Mao H, Fabrichnaya OB, Selleby M, Sundman B (2005) Thermodynamic assessment of the MgO-Al_2O_3-SiO_2 system. Journal of Material Research 20 (4):975-986
72. Jung IH, Decterov SA, Pelton AD (2004) Critical thermodynamic evaluation and optimisation of the MgO-Al_2O_3, CaO-MgO-Al_2O_3, and MgO-Al_2O_3-SiO_2 systems. Journal of Phase Equilibria and Diffusion 25 (4):329-345
73. Jung IH, Decterov SA, Pelton AD (2005) Critical thermodynamic evaluation and optimization of the CaO-MgO-SiO_2 system. Journal of the European Ceramic Society 25:313-333